Journal of the Serbian Chemical Society
JSCS-info@shd.org.rs • www.shd.org.rs/JSCS
J. Serb. Chem. Soc. 78 (5) 741–758 (2013)
JSCS–4454
UDC 550.378+546.791–78+520.84:
550.389(397)
Original scientific paper

Discovery of uranium mineralizations in the rhyolite–granite complex in the Jabal Eghei area of southern Libya

JOVAN KOVAČEVIĆ[1], MEHDI BASHIR TEREESH[2], MIRJANA B. RADENKOVIĆ[3] and ŠĆEPAN S. MILJANIĆ[4]*

[1]Geological Institute of Serbia, P. O. Box 42, 11000 Belgrade, Serbia, [2]Tajoura Nuclear Research Centre. P. O. Box 30878, Tajoura, Libya, [3]University of Belgrade, Vinča Institute of Nuclear Sciences, P. O. Box 522, 11001 Belgrade, Serbia and [4]University of Belgrade, Faculty of Physical Chemistry, P. O. Box 47, 11158 Belgrade 118, Serbia

(Received 19 September, revised 12 November 2012)

Abstract: During an investigation of the Jabal Eghei area in southern Libya and the production of geological maps on a scale of 1:250 000 (Tibesti sector, sheet Wadi Eghei NF 34-1 and NF 34-2), regional prospecting for mineral raw materials was performed. A radiometric survey of the observed targets at the sites indicated two significant uranium mineralizations in rhyolites, and some smaller ones in granites that are in close contact with rhyolites. Rhyolites are located in the central part of the investigated region. They cut through granite rocks. The first mineralization is in the central part of the rhyolite region, which is mostly composed of silificated rhyolites. The second one was discovered near the granite–rhyolite contact zone, characterized by the presence of silicified breccia rocks. These findings were confirmed by laboratory measurements of more than seventy samples collected in the area, using high-resolution gamma-ray spectrometry. The concentrations of uranium in these mineralizations were found to range from approx. 50 mg kg^{-1} to more than 600 mg kg^{-1}. The latter value is about 240 times above the Earth's average. Besides uranium, these measurements have also given concentrations of thorium and potassium. Additional geochemical analysis was performed on samples taken from locations where uranium anomalies were discovered using the ICP-MS technique, in which the concentrations of more than forty elements were determined. The uranium mineralizations are accompanied by increased contents of silver (up to 17 times), arsenic (up to 8 times), molybdenum (up to 50 times), mercury (up to 9 times), and lead (up to 14 times), with regards to the Clark values. These results warrant a continued investigation of this region because of potential interest in the discovery of nuclear mineral raw materials.

Keywords: terrestrial radioactivity; Jabal Eghei; gamma-ray spectrometry; uranium; mineralization; geological map.

* Corresponding author. E-mail: epan@ffh.bg.ac.rs
doi: 10.2298/JSC120919124K

INTRODUCTION

Studies of naturally occurring radioactive materials (NORM) are of great interest to many fields of human activity. They usually involve the determination of the uranium, thorium and potassium contents in rocks and soil, since their natural radioactive isotopes are among the most abundant on Earth. Their radioactivity is dependent on three natural radioactive series: the *uranium series* originating with ^{238}U, the thorium series originating with ^{232}Th, and the actino–uranium series originating with ^{235}U, as well as on the singly occurring potassium isotope ^{40}K. As the ratio of natural uranium isotopes ^{235}U to ^{238}U is very low (0.007), the contribution of ^{235}U to environmental radioactivity is negligible. In terms of their abundances, potassium is considered a major element, having crustal abundance with a Clarke value of 2.5 %, while U and Th occur as trace elements with Clarke values of 2.50 and 13 mg kg^{-1}, respectively.[1]

Natural environmental radiation mainly depends on the content of radionuclides in the outcropping rock. Igneous rocks, especially granites, exhibit higher radioactivity, due to geochemical behavior of the above elements during geogenesis. From a practical point of view, uranium is the most important among them. Granitic rocks can serve as uranium source rocks for secondary areas of uranium enrichment that occurs by movement of groundwater through fractures in these rocks or through porous zones within rocks adjacent to the granitic rocks. It dissolves uranium and transports it to a place favorable for its deposition.

The history of geological investigations of the Tibesti Massif and its surroundings is relatively long. The first explorers reached the Massif in the mid-1860s. The remoteness and general inaccessibility of the area made these investigations much slower and more complicated than those in other parts of Libya. After almost half a century of inactivity, French and Italian military experts produced the first sketches and rough topographic maps of Tibesti in the early 1900s. Significant changes in the approach to geological investigations began when the Industrial Research Center (IRC) of Libya was founded in 1970. As the official institution for systematic geological and mining investigations, the IRC commissioned the production of geologic maps at a scale of 1:250,000. The area of direct interest was essentially not hitherto investigated. This lack of previous data, as well as some significant uranium anomalies indicated by preliminary measurements at the site, makes this renewed investigation particularly important. These measurements at Jabal Eghei were performed in order to detect nuclear mineral resources while collecting geological samples. The radiometric survey of the observed targets was realized using portable instruments.

The main objectives of this work were to: 1) investigate the radioactivity of rhyolite–granitoide rocks in the area of Jabal Eghei – Kangara Massif that originates from uranium, thorium and potassium, 2) advance knowledge of the mining potential of this interesting region, especially regarding uranium and 3) contri-

bute to the establishment of a baseline map of environmental radioactivity levels.[2] With these goals in mind, attention was focused on measurements of the radioactivity of ^{238}U, ^{232}Th and ^{40}K isotopes. They are commonly used to determine contents of the corresponding elements in investigated objects. During the course of this work, however, unusual anomalies in uranium-based radioactivity of the terrain were discovered, and accordingly investigations were extended to several other elements, as well as to the recognition of the rock types and corresponding geological aspects of the area, including the production of a geological map, all based on measurements of numerous geological samples collected during the regional geological mapping of Jabal Eghei (Tibesti sector, sheet Wadi Eghei NF 34-1 and NF 34-2).

The data obtained from gamma spectroscopy measurements was also employed to assess the radiological risk in this area,[2] by calculating the corresponding radiation hazard indices and related quantities, in a way analogous to that recently applied in some similar cases.[3,4]

A combination of terrain work (sample collection and preliminary investigation on site), laboratory measurements (determination of contents of elements), and data analysis and interpretation was applied. It was expected to gather necessary data about geological composition, structure, magmatism, mineralization control factors, geochemical and geophysical characteristics. Based on these data, a rough interpretation of the conditions and characteristics of the mineralization environment could be made. High-resolution gamma-ray spectrometry was used to measure the radioactivity of all the collected samples. From the obtained data, contents of the corresponding elements were calculated. They were additionally checked by ICP-MS (Inductively Coupled Plasma Mass Spectroscopy) analysis for comparison. Same method was used to determine concentrations of about forty other elements appearing in minerals. In the case of potassium, the X-ray fluorescence (XRF) method was used for some samples, in addition to the above techniques.

EXPERIMENTAL

Study area

The investigated area of Jabal Eghei is located in the farthest southeastern part of Libya, near the border with Chad. The area is a part of the Tibesti Mountains massif, which is the largest massif in the Sahara. In a morphological sense, the investigated region belongs to rocky deserts at altitudes between 720 and 1120 m. The main geomorphologic feature of the terrain is a rhyolite mass in its central part. The photograph given in Fig. 1 shows the typical appearance of the mass. The area composed of granitoide rocks is mostly flattened due to Eolian erosion, but there are large prominent ridges made of quartzite, gneiss or scorn. There are also large wades in the northern part, which are most favorable for the movement of field vehicles. The investigated region is characterized by a desert climate, with almost no precipitation. There are no inhabited places in the area or in the wider surroundings of approxi-

mately five hundred kilometers in diameter. The investigated area is about 12 km long and 5 km wide.

Fig. 1. Photograph of the rhyolite region in Jabal Eghei exhibiting anomalous radioactivity.

Sample collection and preparation

A total of 110 samples were collected by geological experts in the second half of 2010, from numerous locations in the specified area (Kangara Massif rhyolite, Jabal Eghei). The quantity of each sample was ≈1 kg. Some samples were rocky, while some were mixtures of rocks and sand. The samples were of different geological composition, including granite, rhyolite, granitoide, silification rhyolite and apilite, depending on the type of the natural stretcher of the area. The collecting of the samples was complicated by the desert environment, lack of communications and the general remoteness of the investigated area.

Radiometric surveys of observed spots on the entire massif of rhyolites (about 60 square kilometers), which lie over granitoide rocks, were realized using either a GR-110 scintillation counter or a portable γ-spectrometer GR-130-minispec (with a sodium iodide detector), both made by Exploranium, Canada. The measured profiles were at a distance of about 1 km from each other, for cases without lithologic changes or radioactive anomalies. Radioactive anomalies were registered at two sites in rhyolites. One of them was an area of 100 m×100 m, the other one the area of 50 m×20 m. At these locations, the sampling points were closer to each other: on average, one sample was analyzed per area of 10 m×10 m.

A selection of about seventy samples, based on a preliminary radiometric survey of observed targets at the sites, was subjected to laboratory measurements. Samples were ground in a ball mill, sieved through the 0.2-mm mesh, dried at a temperature slightly above 100 °C to a constant weight, and then homogenized. Each sample was placed in the standard 450 mL Marinelli beaker, sealed hermetically and stored for at least four weeks before counting, to allow the in-growth of uranium and thorium decay products, and achievement of equilibrium between ^{238}U and ^{232}Th and their respective progeny, *i.e.*, to ensure secular equilibrium between ^{226}Ra and its products.

Counting and radioactivity analysis

Radioactivity was measured using standard gamma spectrometry[5,6] to determine the concentrations of ^{238}U, ^{232}Th and ^{40}K isotopes in the samples. Measurements were performed using a gamma spectrometry system with a high-purity germanium (HPGe) detector (Canberra), having a relative efficiency of 23 % and a resolution of 1.8 keV at the 1332.5 keV ^{60}Co gamma line.

The efficiency calibration was performed using a certified standard reference soil material (MIX-OMH-SZ, National Office of Measures, Budapest), spiked with ^{22}Na, ^{57}Co, ^{60}Co, ^{89}Y, ^{133}Ba and ^{137}Cs in the cylindrical Marinelli beaker geometry.

Other utilized methods

As a rule, gamma spectrometry measurements are very selective and highly reliable for the determination of both isotope concentrations and abundances of the corresponding elements. However, in order to check the results obtained by the radioactivity measurements, these results were compared with those obtained by ICP-MS analysis of all samples for U and Th, and also by XRF analysis of some samples for K, because the ICP-MS method is not at all a reliable for the analysis of potassium. X-Ray fluorescence (XRF) is a method of non-destructive elemental analysis based on the emission of characteristic fluorescent X-rays from a sample excited by high-energy X-rays. The spectral line used for the analysis of potassium was $K\alpha_{1,2}$ at 0.3742 nm. The ICP-MS method was also used for geochemical analysis and characterization of samples exhibiting high uranium concentrations through the contents of more than forty micro elements appearing in them, because the ICP-MS is widely accepted as the most powerful method for the analysis and quantification of trace elements, especially metals. It is based on ionizing the sample with inductively coupled plasma and then using a mass spectrometer to separate and measure those ions. Due to this, its sensitivity is of the order of ng kg^{-1}. It is now commonly used in both environmental analyses and geological applications.

RESULTS AND DISCUSSION

General geological characteristics of the investigated area

During the field investigation of the basement in the Jabal Eghei area, the following types of rocks were recognized: amphibolites, metavulcanites, mica-schists, phyllites, calc-silicates, marbles, graphite-schists, quartz–sericite–chlorite schists, quartz–biotite–garnet–staurolite–muskovite schists, hornblende–plagioclase–epidote schists, quartzites, gneisses, serpentinites and other metamorphic rocks.

The identified mineral associations represent metamorphism of rocks of the Lower Tibestian as a regional metamorphism in the interval from the upper greenschist to the lower amphibolite facies. Contact alterations in the zones of contact between granitoids and metamorphites make the geological setting of the research area even more complicated (schists with wollastonite–idocrase–calcite––diopside association and similar rocks). During the syntectonic intrusion of magmatic rocks, partial mixing of metamorphites and granitoids occurred, which resulted in the formation of the parts of the basement in which metamorphic rocks cannot be distinguished from intrusives. Large masses of gneiss rocks occur frequently in these areas. There are also areas in the peripheral parts of the large post-tectonic granitoid intrusions, where foliation in metamorphic rocks is concordant with contacts between granites and metamorphites.

Magmatic rocks. Constituent parts of the consolidated basement are petrolgically different intrusive magmatic rocks, mostly of granitoid affinity. Synchro-

nous with the collisional events, large plutonic bodies of syntectonic igneous rocks were intruded and shaped. Large post-collisional granitoid intrusives were formed at the end of the Proterozoic and during the Lower Paleozoic.[7] Intrusive magmatic rocks constitute the largest part of the basement. They are spatially related to the central and eastern parts of the area made of metamorphic and magmatic rocks.

Granite. Granite is the most common magmatic rock of the basement. These rocks make discontinuous NNE–SSW-striking zones. Granite has largest extension in the investigation area. In the large granitic bodies, the syntectonic character of the magmatites is reflected by well-developed secondary ruptures, along which shearing occurred. These ruptures are echelons arranged in plan view. Macroscopically, these are leucocratic medium-grained to coarse-grained rocks made of orthoclase, albite, quartz and biotite. Frequent and significant variations in the granite mineral composition, mostly in the peripheral parts of large intrusives, which results in changes in the rock type; thus transitions toward granodiorite and diorite are often noticed.

Rhyolite. Large occurrences of rhyolite were noticed in the central part of sheet NF 34-1. The rhyolite lies above metamorphic and igneous rocks of the basement. As resistant rocks, rhyolites make morphologically conspicuous relief forms. Petrologically, these rocks are rhyolites (and porphyrites) of pinkish, reddish and red–brown color. Scarce phenocrysts of potassium feldspars and spherical grains of quartz lie in a matrix composed of microcrystalline quartz and feldspars.

Based on the identified types of rocks (a description of these rocks was left out due to space shortage), the geological map of the area was constructed.[8] The map is given in Fig. 2.

Gamma-ray measurements and specific activity determinations

The background radiation and the samples were counted for 60,000 seconds. The 63.28 keV ^{234}Th gamma ray line and the 1001.03 ^{234m}Pa gamma ray line were used to determine the ^{238}U activity concentration, although the latter one, which is very weak, could only be used for uranium-rich samples. The ^{232}Th activity concentration was determined using the 338.42 and 911.07 keV ^{228}Ac gamma lines. The activities of ^{40}K were determined directly from the 1460.8 gamma line.

After completion of the measurement, the peak areas in the spectrum were calculated. Following the spectrum analysis, count rates for each detected photopeak and the activity per sample mass (specific activity) for each of the detected nuclides were calculated. The specific activity A (Bq kg^{-1}) of a radionuclide is calculated using the following equation:

$$A = \frac{I(E_\gamma)}{mtP_\gamma(E_\gamma)\varepsilon(E_\gamma)} \quad (1)$$

where $I(E_\gamma)$ is the number of counts in a given peak area, corrected for background peaks of a peak at energy E, t is the counting time (s), m is the mass of the sample (kg), $P_\gamma(E_\gamma)$ is the probability of disintegration with E_γ (transition probability) and $\varepsilon(E_\gamma)$ is the detection efficiency for energy E_γ. Obtained specific activities of ^{238}U, ^{232}Th and ^{40}K are given in Table I.

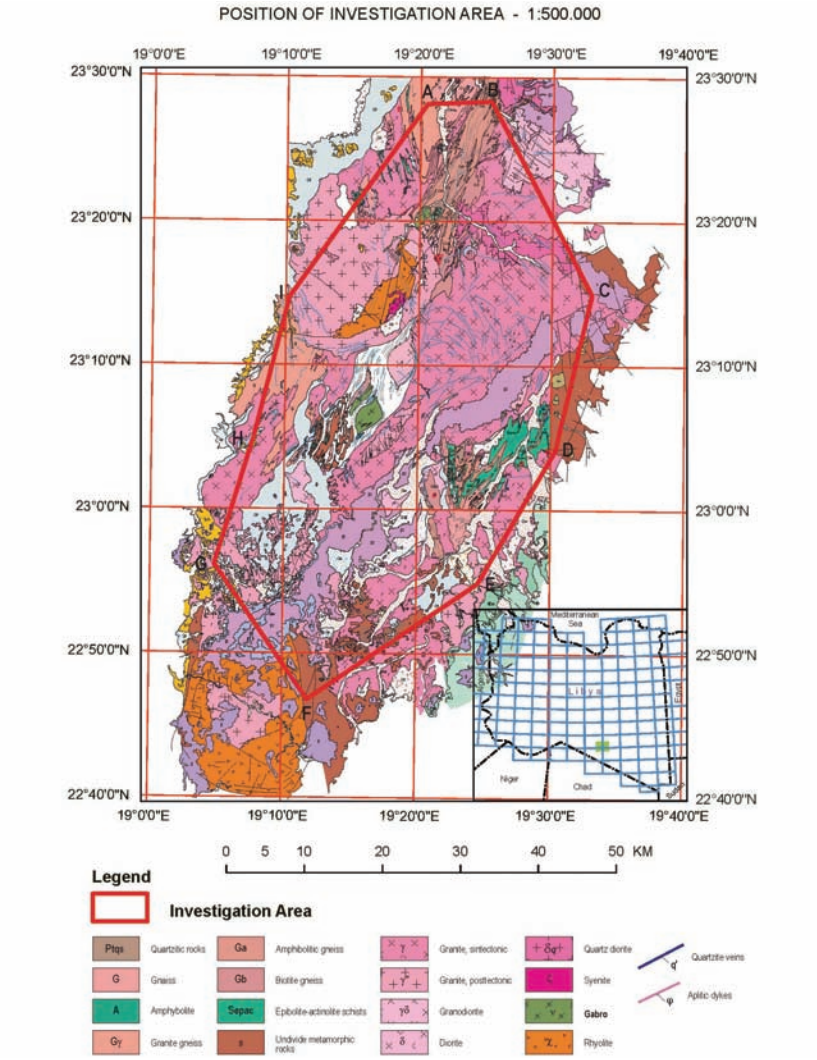

Fig. 2. Geological map of the Jabal Eghei area and the map of Libya with the investigated area highlighted in green.

TABLE I. Specific activities (A / Bq kg^{-1}) of ^{238}U, ^{232}Th and ^{40}K in samples from Jabal Eghei, obtained from gamma spectrometric measurements (values in bold show anomalous radioactivity with regards to the local background level for uranium)

Sample No	Sample Code	^{238}U	^{232}Th	^{40}K	Rock type
1	186	81±15	53±4	1261±76	Rhyolite
2	187	74±10	60±6	1281±86	Rhyolite
3	188	83±12	64±6	1433±94	Rhyolite
4	191	154±21	88±7	1386±86	Granitoide
5	193	125±20	88±7	1462±91	Contact zone q-vein/rhyolite
6	194	64±15	55±5	790±55	q-vein
7	198	91±15	54±5	1170±76	Rhyolite
8	200	87±16	50±5	1157±75	Silificated rhyolite
9	201	99±17	32±4	1763±111	Silificated rhyolite
10	202	177±23	83±7	1591±99	Silificated rhyolite, fault zone
11	203	146±17	147±12	1546±104	Silificated rhyolite
12	205	130±13	101±8	1245±82	Granite
13	207	123±14	96±8	1597±104	Breccia silificated
14	208	180±20	91±8	1749±118	Silificated rhyolite
15	209	377±37	122±9	1155±75	Granite
16	210	173±22	93±7	1513±93	Contact rhyolite–granite
17	211	98±19	81±6	1512±94	Contact rhyolite–granite
18	212	63±13	73±6	1383±86	Rhyolite
19	213	119±19	75±6	1485±94	Rhyolite
20	214	140±13	92±8	1576±100	Rhyolite
21	215	184±24	78±7	1401±89	Rhyolite
22	216	139±16	101±9	1495±99	Silificated rhyolite
23	217	122±14	101±9	1651±109	Contact rhyolite–granite
24	219	140±20	82±7	1067±69	q-breccia
25	220	67±11	129±10	2304±145	Rhyolite
26	222	104±12	71±6	1551±101	Rhyolite
27	223	104±17	80±7	1545±96	Breccia silificated
28	225	69±12	57±5	890±59	Rhyolite
29	226	101±12	82±7	1240±82	Silificated rhyolite
30	227	92±11	85±7	1729±112	Silificated rhyolite
31	230	–	–	–	Rhyolite-breccia
32	231	–	–	–	Rhyolite-breccia
33	234	114±18	59±5	1092±72	Fault zone
34	235	171±23	88±7	1447±92	Rhyolite
35	237	140±14	58±6	561±45	q-breccia
36	238	66±11	24±3	322±25	q-breccia (fault zone)
37	239	98±13	37±3	877±57	Tuff
38	240	284±32	150±11	1517±95	Aplite vein
39	241	448±48	221±15	1210±78	Aplite
40	242	62±14	81±7	1533±97	Silificated rhyolite
41	243	122±18	93±7	1350±86	Silificated rhyolite
42	**244**	**1176±78**	63±7	875±65	Rhyolite
43	**245**	**3097±185**	68±9	529±47	Rhyolite

TABLE I. Continued

Sample No	Code	^{238}U	^{232}Th	^{40}K	Rock type
44	**246**	**3272±194**	64±9	593±50	Rhyolite
45	248	151±14	55±5	995±68	Silificated rhyolite
46	249	62±8	58±5	1048±72	Silificated rhyolite
47	267	64±9	61±6	1148±79	Gabbro
48	268	112±11	55±5	1044±70	Rhyolite
49	269	104±16	43±4	1284±85	Rhyolite
50	270	16±5	11±1	256±20	Silificated rhyolite
51	271	0	14±2	132±13	Silificated rocks
52	272	73±13	62±5	1131±73	Contact rhyolite–granite
53	273	111±16	66±6	1204±78	Amphipolite pyritized
54	274	68±14	64±5	1123±72	Schistose rhyolite
55	275	0	72±7	1120±76	Silificated rhyolite
56	**620**	**1515±98**	26±3	893±67	Rhyolite
57	**621**	**2788±168**	61±9	983±74	Rhyolite
58	**622**	**3570±229**	62±7	750±53	Rhyolite
59	**624**	**7477±458**	0	140±20	q-breccia
60	701	111±13	60±5	1374±88	Rhyolite
61	702	126±14	104±8	1251±76	Granite
62	706	332±33	136±9	1333±83	Granite
63	707	103±12	61±5	1468±94	Rhyolite
64	708	51±8	39±4	777±54	Granite
65	709	182±22	70±6	1296±82	Granite
66	710	184±21	68±6	1288±81	Rhyolite
67	712d	62±12	39±4	1742±106	Granite
68	713	104±16	64±5	1774±108	Rhyolite
69	2775	73±11	63±5	1242±77	Granite
70	2776d	82±15	59±5	1342±83	Rhyolite
71	2778d	147±19	80±6	1451±90	Rhyolite

Concentrations of uranium, thorium and potassium in the samples

Specific activities of radioisotopes given in the above table were converted into concentrations of corresponding elements, according to the following expression:

$$F_{\mathrm{E}} = A_{\mathrm{I}} \frac{M_{\mathrm{I}}}{\lambda_{\mathrm{I}} N_{\mathrm{A}} f_{\mathrm{I}}} C \tag{2}$$

where F_{E} is the fraction of element E in the sample, A_{I} is the measured specific activity of the isotope I (Bq kg^{-1}), M_{I}, λ_{I}, and f_{I} are the atomic mass (kg mol^{-1}), the decay constant (s^{-1}), and the fractional atomic abundance in nature, respectively, of the radioisotope considered, N_{A} is Avogadro's number, while C is a constant with a value of 10^6 for U and Th and 10^2 for K. In this way, elemental concentrations are expressed as mg kg^{-1} for uranium and thorium, and as percen-

tages (%) for potassium. For inter-comparison, these data, together with the results of ICP-MS analysis, and XRF analysis for some samples, were collected and are given in Table II.

TABLE II. Concentrations (*F*) of U, Th and K in samples collected in the Jabal Eghei area

Sample		U concentration, mg kg^{-1}			Th concentration, mg kg^{-1}			K concentration, %	
No	Code	Gamma	ICP-MS	XRF	Gamma	ICP-MS	XRF	Gamma	XRF
1	186	6.5±1.2	1.86		13.0±1.1	11.7		4.16±0.25	
2	187	6.0±0.8	2.38		14.8±1.4	13.3		4.22±0.28	
3	188	6.7±1.0	2.45		15.7±1.5	15.4		4.73±0.31	
4	191	12.4±1.7	6.37		21.8±1.7	22.4		4.57±0.28	
5	193	10.1±1.6	6.12		21.6±1.7	22.9		4.82±0.30	
6	194	5.2±1.2	1.45		13.4±1.2	12.3		2.60±0.18	
7	198	7.3±1.2	2.89		13.4±1.2	11		3.86±0.25	
8	200	7.1±1.3	3.69		12.3±1.1	12.6		3.81±0.25	
9	201	8.0±1.4	0.99		8.0±0.9	5.1		5.82±0.37	
10	202	14.3±1.8	6.29		20.5±1.7	22.7		5.25±0.33	4.7
11	203	11.8±1.4	7.75		36.2±2.9	32.8		5.10±0.34	
12	205	10.6±1.1	4.62		24.9±2.0	21.5		4.10±0.27	
13	207	10.0±1.1	1.63		23.6±2.0	17.5		5.27±0.34	
14	208	14.6±1.6	9.7		22.5±2.1	18.2		5.77±0.39	
15	209	30.6±3.0	21.8		30.1±2.2	28.9		3.81±0.25	3.6
16	210	14.0±1.8	4.21		22.9±1.8	23.5		4.99±0.31	
17	211	7.9±1.5	1.56		19.9±1.6	16.7		4.99±0.31	4.6
18	212	5.1±1.1	1.16		18.0±1.4	17.8		4.56±0.29	
19	213	9.7±1.5	2.14		18.5±1.5	18.2		4.90±0.31	
20	214	11.3±1.1	4.7		22.6±1.9	19.8		5.20±0.33	
21	215	14.9±1.9	7.06		19.3±1.6	16.2		4.62±0.29	
22	216	11.3±1.3	3.67		25.0±2.2	17.1		4.93±0.33	
23	217	9.9±1.1	2.02		24.9±2.2	17.3		5.45±0.36	
24	219	11.3±1.7	2.41		20.3±1.6	14.8		3.52±0.23	
25	220	5.4±0.9	4.7		31.9±2.6	15.7		7.60±0.48	
26	222	8.4±0.9	4.16		17.4±1.6	15.1		5.11±0.33	
27	223	8.4±1.4	1.25		19.6±1.6	13.1		5.10±0.32	
28	225	5.6±1.0	1.55		13.9±1.2	11.3		2.94±0.20	
29	226	8.2±1.0	1.15		20.2±1.8	9.1		4.09±0.27	
30	227	7.4±0.9	3.87		21.1±1.8	5.4		5.70±0.37	
31	230	–	175.5		–	1.43		–	
32	231	–	40.9		–	0.23		–	
33	234	9.2±1.5	4.87		14.6±1.3	18.1		3.60±0.24	
34	235	13.8±1.9	1.6		21.6±1.8	10.7		4.77±0.30	
35	237	11.3±1.2	3.77		14.4±1.5	9.6		1.85±0.15	
36	238	5.4±0.9	1.48		5.9±0.6	4.6		1.06±0.08	
37	239	8.0±1.0	1.11		9.1±0.8	8.5		2.89±0.19	
38	240	23.0±2.6	14.1		36.9±2.7	38.7		5.00±0.31	4.5
39	241	36.3±3.9	21.2		54.5±3.7	72.8		3.99±0.26	3.6
40	242	5.0±1.1	0.12		19.9±1.6	1.4		5.06±0.32	

TABLE II. Continued

Sample		U concentration, mg kg^{-1}			Th concentration, mg kg^{-1}			K concentration, %	
No	Code	Gamma	ICP-MS	XRF	Gamma	ICP-MS	XRF	Gamma	XRF
41	243	9.9±1.5	4.54		22.9±1.8	23.2		4.45±0.28	
42	**244**	**95.3±6.3**	**50.1**	**71.5**	15.5±1.7	10.7	13	2.89±0.21	2.2
43	**245**	**250.9±15.0**	**214**	**208.9**	16.7±2.3	11.6	9.6	1.74±0.15	1.1
44	**246**	**265.0±15.7**	**204**	**208.6**	15.9±2.1	11	8.6	1.96±0.16	1.5
45	248	12.2±1.2	4.69		13.5±1.3	10.5		3.28±0.22	
46	249	5.0±0.7	1.49		14.3±1.3	9.9		3.46±0.24	
47	267	5.2±0.8	2.31		14.9±1.5	12.6		3.79±0.26	
48	268	9.1±0.9	2.52		13.4±1.2	12.3		3.44±0.23	
49	269	8.4±1.3	1		10.5±1.1	7.9		4.23±0.28	
50	270	1.3±0.4	0.44		2.7±0.4	2.7		0.84±0.07	
51	271	0.0±0.0	0.25		3.4±0.5	1.9		0.44±0.04	
52	272	6.0±1.1	1.62		15.4±1.3	14.7		3.73±0.24	
53	273	9.0±1.3	1.6		16.2±1.4	14.2		3.97±0.26	
54	274	5.5±1.1	0.91		15.7±1.3	13		3.71±0.24	
55	275	0.0±0.0	0.45		17.8±1.6	5.7		3.69±0.25	
56	**620**	**122.7±7.9**	**74.2**	**105.8**	6.5±0.7	10.4	10.3	2.95±0.22	2.2
57	**621**	**225.8±13.6**	**149**	**187**	15.1±2.3	11.6	11.2	3.24±0.24	2.2
58	**622**	**289.2±18.5**	**232**	**225.1**	15.3±1.8	12.1	10.4	2.47±0.18	1.9
59	**624**	**605.7±37.1**	**356**	**294.2**	0.00±0.0	2.9	3.1	0.46±0.07	0.1
60	701	9.0±1.0	3.16		14.7±1.4	12.3		4.53±0.29	
61	702	10.2±1.1	10.6		25.6±2.0	56.7		4.13±0.25	
62	706	26.9±2.7	19.95		33.5±2.3	48.1		4.40±0.27	
63	707	8.4±1.0	2.93		15.0±1.3	14.5		4.84±0.31	
64	708	4.2±0.6	1.56		9.7±1.0	12.4		2.56±0.18	
65	709	14.7±1.8	12.4		17.2±1.4	53.9		4.28±0.27	
66	710	14.9±1.7	2.57		16.8±1.4	8.8		4.25±0.27	
67	712d	5.0±1.0	2.08		9.7±0.9	15.1		5.75±0.35	
68	713	8.4±1.3	2.91		15.8±1.3	17.9		5.85±0.36	
69	2775	5.9±0.9	–		15.5±1.2	–		4.09±0.26	
70	2776d	6.7±1.2	–		14.5±1.2	–		4.42±0.27	
71	2778d	11.9±1.6	4.25		19.8±1.5	15.4		4.79±0.30	

Table II is a good illustration of the reliability of the different methods used to determine the elemental concentrations. Undoubtedly, the most reliable among them is gamma spectrometry. The table shows that ICP-MS analysis is in very good agreement with radioactivity measurements for thorium (most results are within 15 %), and in moderately good agreement for uranium; most results are within 60 %, with the ICP values always being lower than the radioactivity ones. However, for potassium, there was almost no agreement at all. This discrepancy was expected, as the relatively low ionization potential of potassium causes its ionization to occur early at the entrance into the plasma. Thus, it is forced by radial electric field on its way through plasma to migrate from the central zone, which means that its concentration in that zone is much lower than the true

concentration. This behavior has an impact on the measurement of potassium concentration. Potassium is not unique among the elements in this behavior in ICP. For this reason, XRF analysis was used to prove undoubtedly the previously obtained results for potassium from gamma spectrometry measurements.

Moreover, it can be notice that the thorium and potassium concentrations given in Tables I and II are, on average, within the background levels, while uranium in some samples (620–622, 624, 244–246; these numbers are given in bold in Tables I and II) is remarkably increased.

As mentioned earlier, a radiometric survey of the observed targets at the sites was performed while collecting the samples. At the same time, the local average background values in cps (counts per second) for different types of rocks were established and are given in Table III. Typically, several thousand measurements, sometimes up to five thousand, were performed for each value of background given in the Table. This survey was the first indication of increased radioactivity of rhyolites through the increased background value. Further laboratory measurements fully proved these findings and it was shown that they come from uranium.

TABLE III. Average background values for various types of rocks in the region of Jabal Eghei, obtained from a radiometric survey of the observed targets at the sites

Rock type	Local background, cps
Granitoide	120
Rhyolite	160
Syenite	125
Quartzite	35
Skarn	40
Amphipolite	45

This survey indicated two significant uranium anomalies in the rhyolites, as well as some smaller ones in granites that are in close contact with rhyolites. These field findings were subsequently confirmed by laboratory measurements.

The rhyolites are located in the central part of the investigated region, covering an area of about 60 square kilometers. They cut through granite rocks. From the viewpoint of nuclear mineral raw materials, rhyolites are always considered as rocks of highest significance.

Anomaly I is located in the central part of the rhyolite region (23°14' 23.2"; 19°17' 04"), which is mostly composed of silificated rhyolites. In an area of size 60 m × 40 m counts from about 500 to above 2400 cps were registered, *i.e.*, significantly above the background level. Those values correspond to sample codes 244–246 and 620–622 (Table II). Using the portable GR-130 γ-spectrometer it was proved that this anomaly could exclusively be attributed to uranium, because corresponding numbers of counts for Th and K were within the back-

ground values for this type of rocks. Experience with this instrument and the way of running the measurements enabled the investigators to estimate roughly the concentration of uranium in mg kg^{-1} from the number of counts per second. The estimations obtained in this manner were substantiated by the three applied laboratory methods. Conclusively, all methods gave very similar results, which clearly confirmed that the studied area is enriched in uranium, if compared to the local background. In some cases, the enrichment was up to two orders of magnitude.

Geochemical analysis

As mentioned above, ICP-MS method was employed in this work in addition to radiological techniques. It was used for geochemical analysis of a limited number of samples from locations where uranium mineralizations (anomaly I) were registered, not only to compare the contents of uranium or thorium with those obtained by gamma spectrometry, but also to determine the concentrations of about forty other elements appearing in the examined minerals. These elements are important for understanding the entire geological context regarding uranium. The obtained results are presented in Table I-S of the Supplementary material to this paper, together with the corresponding Clark values.

Formation of uranium mineralizations is directly related to its geochemical properties and behavior in different geological media. The discovered uranium mineralizations in Jabal Eghei are spatially and genetically connected to granitoid rocks cut through by rhyolites. Based on the geological and structural characteristics of the area, as well as the locations of these uranium mineralizations, and bearing in mind the results of the geochemical analyses (Table I-S – increased contents of As a P), it could be concluded that a hydrothermal stage occurred in their formation. In the initial phase, uranium was bonded mostly with petrogenetic minerals of granitoids (feldspar and biotite). Although the concentration of uranium in these minerals is relatively low, the total amount of uranium bound in the rocks in this way is large, because of the great amounts of these rocks and the carrier mineral within them. Beside traces of uranium in the petrogenetic minerals of magmatic rocks, uranium in them also appears in the form of independent minerals, cationic substitutes in the accessory minerals of granitoid complexes and vulcanites. In waters with pH between 4 and 7.5, complexes of the uranyl ion with $KAsO_4^{2-}$ and SiO_3^{2-} may be, and probably were, formed. In the presence of Na^+, K^+, Ca^{2+}, Mg^{2+} and Fe^{2+}, the solubility of uranyl complexes is decreased. This leads to the formation of more favorable conditions for uranium mineralization. Some of these minerals are insoluble (such as their compounds with PO_4^{3-}, AsO_4^{3-}, SiO_2, *etc.*), thus they appear accompanied with uranium at a location, while the others easily move to the solution.[10]

Anomaly II was discovered near the granite–rhyolite contact zone (23°13'42"; 19°16'05"). This zone is connected with a noticeable tectonic zone.

The azimuth of the zone is 160° and dip 85°. It is characterized by the presence of silicified breccia rocks. Counting in the field gave values from 400 to above 3000 cps. From these measurements, it was estimated that concentrations of uranium were higher than those of the first anomaly. This estimation was further confirmed by laboratory measurements (sample codes 230, 231 and 624) using the already described methods. Simultaneously, the thorium concentrations in these samples were negligible. From the location where this uranium anomaly was registered, three samples were taken for further geochemical analysis for significant elements, similarly to the anomaly 1. The results of the analyses are given in Table II-S of the Supplementary material to this paper.

The results of chemical analysis indicate that the registered uranium mineralizations are accompanied with anomal contents of silver, arsenic, molybdenum, mercury and lead.

Taking into account the location and manner of appearance of these uranium anomalies, the following could be concluded. Uranium was probably deposited from mineralized solutions circulating through granites and rhyolites, especially through the fault zones in them, where geochemical conditions were favorable (clay- and iron-abundant regions). Both types of minerals are known as exceptional absorbers of uranium in nature. Significant concentrations of these minerals, especially limonite, were discovered just in the open structure. Some additional uranium anomalies of lower countings (300 to 500 cps) were discovered within the granitoide massif, very close to rhyolites. They are certainly not of economic interest, but could serve as evidence that the main primary source of uranium mineralization was connected with granitoides. It is to be ascertained why the rocks with increased concentrations of uranium do not contain more thorium than the average background. This could be an indication of preferable deposition of uranium to its washing at such points.

Thorium appearances. In the investigated area, the greater part with increased contents of thorium (30 to 72 mg kg^{-1}) were found in granitoide rocks, very close to the granitoide–rhyolite contact zone, on the western side of rhyolites. They are not of interest because of the very low intensities of mineralization.

Potassium. Taking into account that the average concentration of potassium in the Earth's crust is about 2.5 % and in magmatic rocks 3.3 %, the results shown in Table II give an indication of increased contents of this element in the Jabal Eghei rhyolites and granitoide rocks. The most important carriers of uranium are primary calc-alkaline and alkaline acidic magmas, in which potassium prevails over sodium. Uranium concentrations are decreased going toward more alkaline and calcium–magnesium types of granitoide complexes.

A simple genetic model for uranium mineralization in the Jabal Eghei region

The main primary sources of uranium mineralization are granitoides. Uranium is mobilized from them mostly through cold solutions and deposited in favorable geochemical environments, such as contact zones with rhyolites, fault structures filled with clay, ferrous oxides *etc*. During the phase of magma differentiation, uranium was predominantly bonded to petrogenic minerals, such as feldspars and biotites.[11] Although the uranium concentration in these minerals is relatively low (*e.g*., in feldspars, the average concentration is 10^{-6} %), the total amount of uranium in these rocks is large, due to their great masses. On the other hand, concentrations of uranium in micas (which are basically biotites) are about five times higher than the average ones in magmatic rocks. This could also be of importance for the ore deposits. Besides the presence of uranium traces in petrogenetic minerals of magmatic rocks, uranium is also present in the form of independent minerals, as well as on the surfaces of crystals.

Regarding the genesis of the ore deposits and the possibilities of the formation of economically interesting uranium concentrations, which are spatially and genetically related to acidic and intermediate magmatic complexes, the leaching of uranium is of particular interest. It is connected with the possibilities of uranium mobilization from primary sources and its concentration in media to be transported to locations of mineralization. Under favorable physicochemical and geochemical conditions, theoretically about 40 % of total uranium could be mobilized from granitoide complexes. In aqueous solutions, uranium can be often found in the form of sulfate, carbonate, phosphate, chloride and fluoride complexes. The chemical stability of these species predominately depends on the pH and *Eh* values, temperature and the physicochemical properties of the ore-bearing fluids. Numerous factors could have had an impact on the uranium mineralization from ore-bearing solutions and the appearance of its mineralization in the rhyolite massif, such as changes in its chemical composition, or the degassing of solutions in chemical reactions with rock complexes while traveling through rhyolites. The most important factors that lead to the uranium mineralization are changes in pH and *Eh* values, as well as changes in the CO_2 concentration along the route of the ore-bearing solutions from granite to rhyolites.

Bearing in mind all the collected data, connection between uranium mineralization and tecto–magmatic (*i.e*., tecto–volcanic) structures, or more specifically – effusive, volcanic and sub-volcanic structures could be assumed. This further means that the possibility of volcanic uranium mineralization should not be excluded. Uranium mineralization is spatially and genetically related to the volcanic complexes (rhyolites). Some interesting data about the Tibesti massif generally, as well as about Jabal Eghei area, related to this issue have already been published in the scientific literature.[12,13] The spatial position of the postorogen magmatism, which is at the same time the lithologic control factor of the

mineralization position, is controlled by the locations of deep fault zone cross sections. The forms of the ore bodies depend on the structural and lithologic control factor. The uranium ore bodies in anomaly I were probably in the form of a pillar (column). The main ore material was pitchblende, although the presence of uranitite, coffinite and uranium titanite could not be excluded. A full explanation of the genesis of these uranium mineralizations could be obtained from detailed geological investigations.

The possible positions and forms of the ore bodies, as well as a model of the formation of uranium mineralizations are shown in Fig. 3.

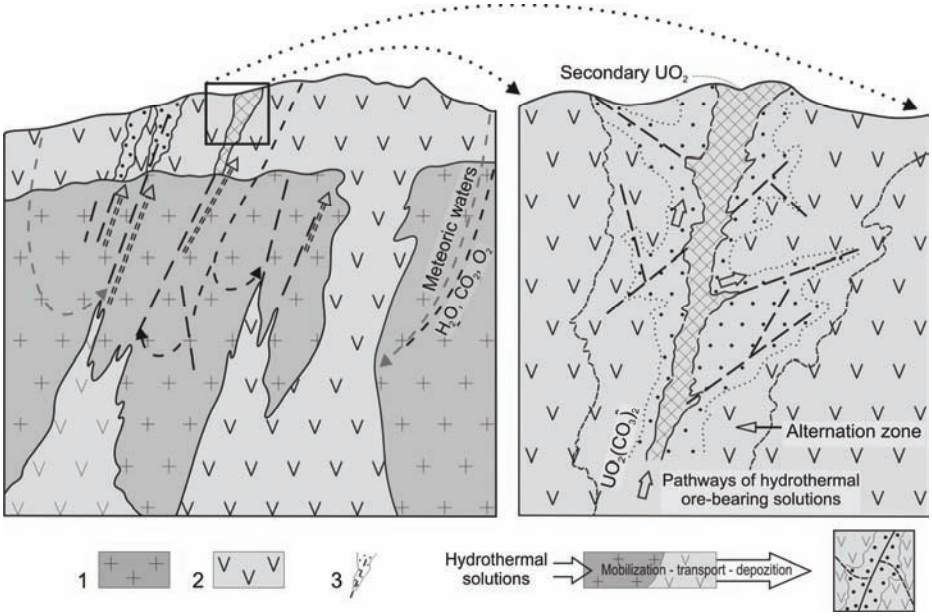

Fig. 3. Schematic representation of the genetic model of uranium mineralization in rhyolites in the Jabal Eghei region: 1 – granitoide rocks; 2 – rhyolites; 3 – uranium mineralization.[7] The side length of the square is 300 m.

CONCLUSIONS

This investigation of the terrain of Jabal Eghei in southern Libya represents the first systematic sampling and radioactivity measurements, and the first determinations of concentrations of some important elements.

Two significant uranium anomalies-mineralizations were discovered in the area, while thorium and potassium were found to be at the average background level, except in a minor number of slightly increased samples.

Geochemical analysis of some samples, taken from places where uranium anomalies were discovered, for more than forty elements was realized using the ICP-MS technique, for a better insight into these anomalies.

Based on all investigations of Jabal Eghei, a detailed geological map of the area was drawn.

In our opinion, investigation of this interesting region, primarily its part made of rhyolites, should be continued, because that might be of interest for the discovery of nuclear mineral raw materials.

SUPPLEMENTARY MATERIAL

Results of geochemical (ICP-MS) analysis of rhyolites exhibiting increased ura¬nium values – anomalies I and II, are available electronically from http://www.shd.org.rs/JSCS/, or from the corresponding author on request.

Acknowledgments. This investigation was realized under the contract between the Industrial Research Centre (IRC) from Tajoura (Libya) and the Geological Institute of Serbia (GIS) from Belgrade (Serbia). The authors are grateful to the IRC for providing the samples analyzed in this work, as well as for permission to publish the obtained data.

И З В О Д

ОТКРИЋЕ УРАНИЈУМСКИХ МИНЕРАЛИЗАЦИЈА У РИОЛИТСКО-ГРАНИТСКОМ КОМПЛЕКСУ У ОБЛАСТИ *JABAL EGHEI* У ЈУЖНОЈ ЛИБИЈИ

ЈОВАН КОВАЧЕВИЋ[1], МЕХДИ БАШИР ТЕРЕШ[2], МИРЈАНА Б. РАДЕНКОВИЋ[3] и ШЋЕПАН С. МИЉАНИЋ[4]

[1]Геолошки институт Србије, п.пр. 42, 11000 Београд, [2]Tajoura Nuclear Research Centre, P. O. Box 30878, Tajoura, Libya, [3]Универзитет у Београду, Институт за нуклеарне науке „Винча“,п.пр. 522, 11001 Београд и [4]Универзитет у Београду, Факултет за физичку хемију, п.п. 47, 11158 Београд

Током истраживања подручја *Jabal Eghei* у јужној Либији и прављења геолошких мапа размере 1:250.000 (сектор Тибести, лист Вади Еги НФ 34-1 и НФ 34-2), урађена је регионална проспекција за минералне сировине. Радиометријски преглед појединих тачака на терену указао је на две значајне уранијумске минерализације у риолитима, као и на неколико мањих у гранитима који су у блиском контакту с риолитима. Риолити су лоцирани у централном делу истраживаног подручја. Они пробијају гранитне стене. Прва минерализација је у средишњем делу риолитске области, која се углавном састоји од силификованих риолита. Друга је откривена близу контактне зоне гранити–риолити, коју карактерише присуство силификованог бреча. Ови су налази потврђени лабораторијским мерењима на више од седамдесет узорака прикупљених у овој области, коришћењем гама спектрометрије високе резолуције. Нађено је да се концентрације уранијума у овим минерализацијама крећу од око 50 mg kg^{-1} до више од 600 mg kg^{-1}. Потоња вредност је око 240 пута већа од средње вредности на Земљи. Поред уранијума, ова мерења су дала концентрације торијума и калијума. Додатне геохемијске анализе су урађене на узорцима са локација на којима су откривене уранијумске аномалије коришћењем технике ICP-MS, у којима су одређене концентрације више од четрдесет елемената. Уранијумске минерализације су праћене повећаним садржајима сребра (до 17 пута), арсена (до 8 пута), молибдена (до 50 пута), живе (до 9 пута) и олова (до 14 пута), у односу на Кларкове вредности. Добијени резултати заслужују да се настави истраживање ове области, зато што постоји могућност да се овде открију нуклеарне минералне сировине.

(Примљено 19. септембра, ревидирано 12.новембра 2012)

REFERENCES

1. V. I. Vernadskiĭ, *Ocherki geohimii*, Nauka, Moskva, Russia, 1983 (In Russian)
2. M. B. Tereesh, M. B. Radenkovic, J. Kovacevic, S. S. Miljanic, *J. Radiat. Prot. Dosim.* **153** (2013) 475
3. R. O. Bastos, C. R. Appoloni, *Radioactivity of rocks from the geological formations belonging to the Tibagi River hydrographic Basin*, in *2009 International Nuclear Atlantic Conference – INAC*, Rio de Janeiro, Brazil, 2009
4. R. C. Ramola, V. M. Choubey, G. Prasad, G. S. Gusain, Z. Tosheva, A. Kies, *Curr. Sci.* **100** (2011) 906
5. G. R. Gilmore, *Practical Gamma-Ray Spectrometry*, 2nd ed., Wiley, Warrington, UK, 2008
6. G. E. Knoll, *Radiation Detection and Measurement*, 3rd ed., Wiley, New York, USA, 2000
7. A. A. Makhrouf, *Geology, petrology, geochemistry, and geochronology of Eghei (Nugay) batholith alkali rich granites, NE Tibesti, Libya*, University of North Carolina at Chapel Hill, Chapel Hill, USA, 1984
8. M. Toljić, J. Kovačević, *Geological map of Libya 1:250,000; Sheet Wadi Eghei NF 34-1*, in *General Report (Mineral raw materials)*, Industrial Research Center, Tripoli, Libya and the Geological Institute of Serbia, Belgrade, Serbia, 2010, p. 264
9. A. A. Beus, S. V. Grigorian, *Geochemical exploration methods for mineral deposits*, Applied Publishing, Wilmette, USA, 1977
10. S. M. Romberger, *Transport and deposition of uranium in hydrothermal systems at temperatures up to 300 °C: Geological implications*, in *Uranium geochemistry, mineralogy, geology, exploration and resources*, B. De Vivo, Ed., The Institution of Mining and Metallurgy, London, UK, 1984, pp. 12–17
11. M. Moreau, *L'uranium et les granitoides–essai d'interpretation (in French)*, in *Geology, mining, and extractive processing of uranium*, M. J. Jones, Ed., Institution of Mining Metallurgy, London, UK, 1977, pp. 83–102.
12. I. B. Suayah, J. S. Miller, B. V. Miller, T. M. Bayer, J. J. W. Rogers, *Afr. Earth. Sci.* **44** (2006) 561
13. A. A. Makkrouf, *J. Afr. Earth. Sci. (and the Middle East)* **7** (1988) 945.